

---

Nuclear Photon Science  
**Hadron Nuclear Physics (HNP06)**  
 February 16-18 (2006), JAEA, Kizu, Japan

---

## PHENOMENOLOGICAL STUDY FOR THE $\Theta^+$ AND TWO-MESON COUPLING

TETSUO HYODO\* AND ATSUSHI HOSAKA

*Research Center for Nuclear Physics (RCNP) Ibaraki 567-0047, Japan*

*E-mail: hyodo@yukawa.kyoto-u.ac.jp*

\* *Present address: Yukawa Institute for Theoretical Physics, Kyoto University, Kyoto 606-8502, Japan*

We examine several assignments of spin and parity for the pentaquark  $\Theta^+$  state ( $J^P = 1/2^\pm, 3/2^\pm$ ) in connection with phenomenology of known baryon resonances, using a general framework based on the flavor symmetry. Assuming that the  $\Theta^+$  belongs to an antidecuplet representation which mixes with an octet, we calculate the mass spectra of the flavor partners of the  $\Theta^+$  based on the SU(3) symmetry. The decay widths of the  $\Theta^+$  and nucleon partners are analyzed for the consistency check of the mixing angle obtained from the masses. It is found that a suitable choice of the mixing angle successfully reproduces the observed masses of exotics, when their spin and parity are assigned to be  $J^P = 3/2^-$ , together with other nonexotic resonances of  $J^P = 3/2^-$ . The decay widths of  $\Theta \rightarrow KN$ ,  $N(1520) \rightarrow \pi N$ , and  $N(1700) \rightarrow \pi N$  are also reproduced simultaneously. We then evaluate two-meson couplings of  $\Theta^+$ , using experimental information of nucleon partners decaying into  $\pi\pi N$  channels, in which the two pions are in scalar- and vector-type correlations. We examine two assignments of spin and parity  $J^P = 1/2^+$  and  $3/2^-$ , for which the experimental spectra of known resonances with exotic baryons are properly reproduced by an octet-antidecuplet representation mixing scheme. Using the obtained coupling constants, total cross sections of the reactions  $\pi^- p \rightarrow K^- \Theta^+$  and  $K^+ p \rightarrow \pi^+ \Theta^+$  are calculated. Substantial interference of two terms may occur in the reaction processes for the  $J^P = 1/2^+$  case, whereas the interference effect is rather small for the  $3/2^-$  case.

### 1 Introduction

In this article, we would like to discuss two topics; one is the representation mixing scheme to study the properties of the exotic state with the flavor SU(3)

symmetry<sup>1</sup>, and the other is the two-meson coupling of the  $\Theta^+$  based on the mixing scheme<sup>2</sup>. The former is reported in section 2 and the latter is discussed in section 3.

In order to study the exotic particles, it is important to consider simultaneously other members with nonexotic flavors in the same SU(3) multiplet which the exotic particles belong to. The identification of the flavor multiplet provides the foundation of the model calculation, for instance, in order to construct effective interaction Lagrangians, or to construct wave functions in the constituent quark models. In addition, when we successfully determine the flavor multiplet, the spin and parity  $J^P$  of exotic states can be specified by the identified non-exotic partners whose  $J^P$  is known. Since the SU(3) flavor symmetry with its breaking governs the relations among hadron masses and interactions<sup>3</sup>, we naively expect that the exotic states also follows the symmetry relations. In other words, the existence of exotic particles would require the flavor partners, if the flavor SU(3) symmetry plays the same role as in the ordinary three-quark baryons.

In this study, we assume that  $\Theta(1540)$ <sup>4</sup> and  $\Xi_{3/2}(1860)$ <sup>5</sup> do exist at these energies, despite the controversial situation of experiments. Although we use these specific mass values, the symmetry relations we derive here are rather general, and can be applied to other exotic states once they are assumed to belong to the same SU(3) representations. Therefore, when any other exotic particles (with the quantum number of  $\Theta^+$  or  $\Xi_{3/2}$ ) are found experimentally in future, we can immediately apply the present formulae to these states.

Concerning the representation that the  $\Theta^+$  belongs to, there are several conjectures in model calculations. In the chiral soliton models<sup>6</sup>, the  $\Theta^+$  and  $\Xi_{3/2}$  belong to the antidecuplet ( $\overline{10}$ ) representation with spin and parity  $J^P = 1/2^+$ . An interesting proposal was made by Jaffe and Wilczek<sup>7</sup> in a quark model with diquark correlation. The model is based on the assumption of the strong diquark correlation in hadrons and the representation mixing of an octet ( $8$ ) with an antidecuplet ( $\overline{10}$ ). The attractive diquark correlation in the scalar-isoscalar channel leads to  $J^P = 1/2^+$  for the  $\Theta^+$ . With the ideal mixing of  $8$  and  $\overline{10}$ , in which states are classified by the number of strange and anti-strange quarks,  $N(1710)$  and  $N(1440)$  resonances are well fit into members of the multiplet together with the  $\Theta^+$ . However, it was pointed out that mixing angles close to the ideal one encountered a problem in the decay pattern of  $N(1710) \rightarrow \pi N$  and  $N(1440) \rightarrow \pi N$ . Rather, these decays implied a small mixing angle<sup>8,9,10</sup>. This is intuitively understood by the discrepancy between the broad decay width of  $N(1440) \rightarrow \pi N$  and the narrow decay widths of  $N(1710) \rightarrow \pi N$  and  $\Theta \rightarrow KN$ <sup>11,8</sup>.

At this stage, it is worth noting that the flavor SU(3) symmetry itself does not constrain the spin and parity. Therefore, employing the  $\mathbf{8}-\overline{\mathbf{10}}$  mixing scenario which is the minimal scheme to include the  $\Theta^+$  and  $\Xi^{--}$ , here we examine the possibilities to assign other quantum numbers, such as  $1/2^-$ ,  $3/2^+$ ,  $3/2^-$ , and search for proper nucleon partners of the exotic states among the known resonances. Although the mass formulae were already given previously, they are applied mainly to the  $J^P = 1/2^+$  case in accordance with the Jaffe-Wilczek model<sup>7</sup>, and sometimes to the  $J^P = 1/2^-$ . The spin  $3/2$  states are rarely examined. This is natural because the lower spin states are expected to be lighter. However, once again, the flavor symmetry is nothing to do with the spin and parity by itself, therefore we investigate the  $J^P = 3/2^\pm$  states as well. Indeed, we find a natural solution consistent with both the masses and widths in the  $3/2^-$  case.

The present study is based on the flavor SU(3) symmetry, experimental mass spectra and decay widths of the  $\Theta^+$ , the  $\Xi^{--}$  and known baryon resonances. Hence, the analysis is rather phenomenological, but does not rely upon any specific models. For instance, we do not have to specify the quark contents of the baryons. Although the exotic states require minimally five quarks, nonexotic partners do not have to. Instead, we expect that the resulting properties such as masses and decay rates reflect information from which we hope to learn internal structure of the baryons.

Now, a particularly interesting property that is expected to be characteristic for exotic baryons is their strong coupling to two-meson states in transitions to an ordinary baryon, as studied in Refs. 12,13. Studying two-meson couplings of the exotic baryon  $\Theta^+$  is important for the following reasons.

First, a heptaquark model has been proposed in the early stage of the study of the  $\Theta^+$  to explain a light mass and a narrow decay width<sup>14,15,16,17,18</sup>. Although a quantitative study—in particular with a model of hadrons where  $\Theta^+$  is regarded as a bound state of  $\pi K N$  system—does not make self-bound system with the present knowledge of hadron interactions, a two-meson contribution to the self-energy of  $\Theta^+$  has been shown to be consistent with the expected pattern of the masses of the antidecuplet members<sup>13</sup>.

Second, the importance of two-meson coupling has been implied from an empirical observation of the generalized OZI rule<sup>19</sup>. The dominance of connected quark lines favors creation of a  $q\bar{q}$  pair in the transition of  $\Theta^+(qqqq\bar{q}) \rightarrow N(qqq)$ , which is naturally associated with couplings to two mesons. On the other hand, couplings to a single meson, which are called as “fall apart” decay, should be suppressed, since the final states are not connected by the quark line.

Finally, two-meson couplings play important roles in reaction studies. Without two-meson couplings, all the amplitudes for  $\Theta^+$  production are proportional to the  $\Theta^+KN$  coupling, which is fixed by the very small decay width of the  $\Theta^+$ . However, two-meson couplings are determined from other sources as we will see in the following, independently of the  $\Theta^+KN$  coupling. Therefore, even with the extremely narrow width of  $\Theta^+$ , a sizable cross section can be obtained with two-meson couplings.

In Ref. 13, an analysis of the two-meson coupling was performed in the study of the self-energy of the  $\Theta^+$ , assuming that  $J^P = 1/2^+$  with  $N(1710) \equiv N^*$  in the same antidecuplet ( $\overline{10}$ ). Since the  $\Theta^+$  cannot decay into  $K\pi N$  channel, the coupling constants were determined from the  $N^*$  decay into the  $\pi\pi N$  channel and flavor SU(3) symmetry. Two types of Lagrangians were found to be important for the self-energy of the baryon antidecuplet. It was also shown that the two-meson contribution was indeed dominant over a single-meson contribution. However, the assumption of pure  $\overline{10}$  for  $\Theta$  and  $N^*$  may not be the case in reality.

Now we can improve this point based on the study of the representation mixing, where we find reasonable fits for  $J^P = 1/2^+$  and  $3/2^-$ . Therefore, here we would like to calculate the two-meson couplings including the representation mixing. First we determine the coupling constants of  $N^* \rightarrow \pi\pi N$  from the experimental widths and separate the  $\overline{10}$  component from the  $\mathbf{8}$  component. Then, by using SU(3) symmetry, the coupling constants of  $\Theta K\pi N$  are determined for  $J^P = 1/2^+$  and  $3/2^-$ , including representation mixing of  $\mathbf{8}$  and  $\overline{10}$ . We focus on the decay channels in which the two pions are correlated in scalar-isoscalar and vector-isovector channels, which are the main decay modes of the resonances and play a dominant role in the  $\Theta^+$  self-energy<sup>13</sup>.

As an application of the effective interaction of  $\Theta K\pi N$ , we perform the analysis of the  $\pi^-p \rightarrow K^-\Theta^+$  and  $K^+p \rightarrow \pi^+\Theta^+$  reactions. These reactions were studied using effective Lagrangian approaches<sup>20,21,22,23</sup>. Experiments for  $\pi^-p \rightarrow K^-\Theta^+$  have been performed at KEK<sup>24</sup>, and a high-resolution experiment for the  $K^+p \rightarrow \pi^+\Theta^+$  reaction is ongoing. We can compare the results with these experiments, which may help to determine the  $J^P$  of the  $\Theta^+$ .

## 2 Flavor multiplet of the $\Theta^+$

### 2.1 Analysis with pure antidecuplet

First we briefly discuss the case where the  $\Theta^+$  belongs to pure  $\overline{10}$  without mixing with other representations. In this case, the masses of particles be-

longing to the  $\overline{\mathbf{10}}$  can be determined by the Gell-Mann–Okubo (GMO) mass formula

$$M(\overline{\mathbf{10}}; Y) \equiv \langle \overline{\mathbf{10}}; Y | \mathcal{H} | \overline{\mathbf{10}}; Y \rangle = M_{\overline{\mathbf{10}}} - aY, \quad (1)$$

where  $Y$  is the hypercharge of the state, and  $\mathcal{H}$  denotes the mass matrix. Note that at this point the spin and parity  $J^P$  are not yet specified. The quantum numbers will be assigned as explained below.

In Eq. (1), there are two parameters,  $M_{\overline{\mathbf{10}}}$  and  $a$ , which are not determined by the flavor SU(3) symmetry. However, we can estimate the values of these parameters by considering their physical meaning in some models. For instance, in a constituent quark model,  $\overline{\mathbf{10}}$  can be minimally expressed as four quarks and one antiquark. Therefore,  $M_{\overline{\mathbf{10}}}$  should be at least larger than the masses of three-quark baryons. In this picture, the mass difference of  $\Xi(ssqq\bar{q})$  and  $\Theta(qqq\bar{s})$ , namely  $3a$ , is provided by the difference between the constituent masses of the light ( $ud$ ) and strange quarks, which is about 100-250 MeV<sup>13</sup>. On the other hand, in the chiral quark soliton model,  $3a$  is related to the pion nucleon sigma term<sup>25</sup>. In this picture  $3a$  can take values in the range of 300-400 MeV, due to the experimental uncertainty of the pion nucleon sigma term  $\Sigma_{\pi N} = 64\text{--}79$  MeV<sup>26,27</sup>. Note that in the chiral soliton model, spin and parity are assigned as  $J^P = 1/2^+$  for the antidecuplet.

Taking the above estimation into consideration, we test several parameter sets fixed by the experimentally known masses of particles. The results are summarized in Table 1. We use the mass of the  $\Theta^+$   $M_\Theta = 1540$  MeV and pick up a possible nucleon resonance. Assuming that the  $\Theta^+$  and the nucleon resonance are in the same SU(3) multiplet, the  $J^P$  of the multiplet is determined by that of the nucleon partner. In the three cases of  $J^P = 1/2^+, 3/2^\pm$ , the exotic  $\Xi$  resonance is predicted to be higher than 2 GeV, and the inclusion of  $\Xi(1860)$  in the same multiplet seems to be difficult. Furthermore, the  $\Sigma$  states around 1.8-1.9 GeV are not well assigned (either two-star for  $J^P = 1/2^+$ , or not seen for  $J^P = 3/2^\pm$ ). Therefore, fitting the masses in the pure antidecuplet scheme seems to favor  $J^P = 1/2^-$ .

Next we study the decay widths of the  $N^*$  resonances with the above assignments. For the decay of a resonance  $R$ , we define the dimensionless coupling constant  $g_R$  by

$$\Gamma_R \equiv g_R^2 F_I \frac{p^{2l+1}}{M_R^{2l}}, \quad (2)$$

where  $p$  is the relative three momentum of the decaying particles in the resonance rest frame,  $l$  is the angular momentum of the decaying particles,  $\Gamma_R$  and  $M_R$  are the decay width and the mass of the resonance  $R$ .  $F_I$  is the isospin

Table 1. Summary of subsection 2.1. Masses and  $\Theta^+$  decay widths are shown for several assignments of quantum numbers. For  $1/2^-$  the masses of  $\Theta$  and  $\Xi_{3/2}$  are the input parameters, while for  $1/2^+, 3/2^\pm$ , the masses of  $\Theta$  and  $N$  are the input parameters. Values in parenthesis are the predictions, and we show the candidates to be assigned for the states. All values are listed in units of MeV.

$J^P$	$M_\Theta$	$M_N$	$M_\Sigma$	$M_\Xi$	$\Gamma_\Theta$
$1/2^-$	1540	[1647]	[1753]	1860	$156.1^{+90.8}_{-73.3}$
		$N(1650)$	$\Sigma(1750)$		
$1/2^+$	1540	1710	[1880]	[2050]	$7.2^{+15.3}_{-4.6}$
			$\Sigma(1880)$	$\Xi(2030)$	
$3/2^+$	1540	1720	[1900]	[2080]	$10.6^{+7.0}_{-5.0}$
			-	-	
$3/2^-$	1540	1700	[1860]	[2020]	$1.3^{+1.2}_{-0.9}$
			-	$\Xi(2030)$	

factor (2 for  $\Theta \rightarrow KN$  and 3 for  $N^* \rightarrow \pi N$ ). Assuming flavor SU(3) symmetry, a relation between the coupling constants of  $\Theta \rightarrow KN$  and  $N^* \rightarrow \pi N$  is given by:

$$g_{\Theta KN} = \sqrt{6}g_{N^* \pi N}. \quad (3)$$

With these formulae (2) and (3), we calculate the decay width of the  $\Theta^+$  from that of  $N^* \rightarrow \pi N$  of the nucleon partner. Results are also shown in Table 1. We quote the errors coming from experimental uncertainties in the total decay widths and branching ratios, taken from the Particle Data Group (PDG)<sup>28</sup>. It is easily seen that as the partial wave of the two-body final states becomes higher, the decay width of the resonance becomes narrower, due to the effect of the centrifugal barrier. Considering the experimental width of the  $\Theta^+$ , the results of  $J^P = 3/2^-, 3/2^+, 1/2^+$  are acceptable, but the result of the  $J^P = 1/2^-$  case, which is of the order of hundred MeV, is unrealistic.

In summary, it seems difficult to assign the  $\Theta^+$  in the pure antidecuplet  $\overline{\mathbf{10}}$  together with known resonances of  $J^P = 1/2^\pm, 3/2^\pm$ , by analyzing the mass and width simultaneously.

## 2.2 Analysis with octet-antidecuplet mixing

In this section we consider the representation mixing between  $\overline{\mathbf{10}}$  and  $\mathbf{8}$ . Here we work under the assumption of minimal  $\mathbf{8}$ - $\overline{\mathbf{10}}$  mixing. The nucleon and  $\Sigma$  states in the  $\mathbf{8}$  will mix with the states in the  $\overline{\mathbf{10}}$  of the same quantum numbers. Denoting the mixing angles of the  $N$  and the  $\Sigma$  as  $\theta_N$  and  $\theta_\Sigma$ , the

physical states are represented as

$$\begin{aligned} |N_1\rangle &= |\mathbf{8}, N\rangle \cos \theta_N - |\overline{\mathbf{10}}, N\rangle \sin \theta_N, \\ |N_2\rangle &= |\overline{\mathbf{10}}, N\rangle \cos \theta_N + |\mathbf{8}, N\rangle \sin \theta_N, \end{aligned} \quad (4)$$

$$\begin{aligned} |\Sigma_1\rangle &= |\mathbf{8}, \Sigma\rangle \cos \theta_\Sigma - |\overline{\mathbf{10}}, \Sigma\rangle \sin \theta_\Sigma, \\ |\Sigma_2\rangle &= |\overline{\mathbf{10}}, \Sigma\rangle \cos \theta_\Sigma + |\mathbf{8}, \Sigma\rangle \sin \theta_\Sigma. \end{aligned} \quad (5)$$

To avoid redundant duplication, the domain of the mixing angles is restricted in  $0 \leq \theta < \pi/2$ , and we will find solutions for  $N_1$  and  $\Sigma_1$  lighter than  $N_2$  and  $\Sigma_2$ , respectively.

When we construct  $\overline{\mathbf{10}}$  and  $\mathbf{8}$  from five quarks, the eigenvalues of the strange quark (antiquark) number operator  $n_s$  of nucleon states become generally fractional. However, in the scenario of the ideal mixing of Jaffe and Wilczek, the physical states are given as

$$\begin{aligned} |N_1\rangle &= \sqrt{\frac{2}{3}} |\mathbf{8}, N\rangle - \sqrt{\frac{1}{3}} |\overline{\mathbf{10}}, N\rangle, \\ |N_2\rangle &= \sqrt{\frac{2}{3}} |\overline{\mathbf{10}}, N\rangle + \sqrt{\frac{1}{3}} |\mathbf{8}, N\rangle, \end{aligned}$$

such that  $\langle N_1 | n_s | N_1 \rangle = 0$  and  $\langle N_2 | n_s | N_2 \rangle = 2$ . In this case, the mixing angle is  $\theta_N \sim 35.2^\circ$ . In the Jaffe-Wilczek model,  $N(1440)$  and  $N(1710)$  are assigned to  $N_1$  and  $N_2$ , respectively. Notice that the separation of the  $s\bar{s}$  component in the ideal mixing is only meaningful for mixing between five-quark states, while the number of quarks in the baryons is arbitrary in the present general framework.

### 2.3 Mass spectrum

Let us start with the GMO mass formulae for  $\overline{\mathbf{10}}$  and  $\mathbf{8}$ :

$$M(\overline{\mathbf{10}}; Y) \equiv \langle \overline{\mathbf{10}}; Y | \mathcal{H} | \overline{\mathbf{10}}; Y \rangle = M_{\overline{\mathbf{10}}} - aY, \quad (6)$$

$$M(\mathbf{8}; I, Y) \equiv \langle \mathbf{8}; I, Y | \mathcal{H} | \mathbf{8}; I, Y \rangle = M_{\mathbf{8}} - bY + c \left[ I(I+1) - \frac{1}{4}Y^2 \right], \quad (7)$$

where  $Y$  and  $I$  are the hypercharge and the isospin of the state. Under representation mixing as in Eqs. (4) and (5), the two nucleons ( $N_{\mathbf{8}}, N_{\overline{\mathbf{10}}}$ ) and the two sigma states ( $\Sigma_{\mathbf{8}}, \Sigma_{\overline{\mathbf{10}}}$ ) mix, and their mass matrices are given by  $2 \times 2$  matrices. The diagonal components are given by Eqs. (6) and (7), while the off-diagonal elements are given as

$$\langle \mathbf{8}, N | \mathcal{H} | \overline{\mathbf{10}}, N \rangle = \langle \mathbf{8}, \Sigma | \mathcal{H} | \overline{\mathbf{10}}, \Sigma \rangle \equiv \delta.$$

Table 2. Parameters for  $1/2^+$  case. All values are listed in MeV except for the mixing angles.

$M_{\mathbf{8}}$	$M_{\overline{\mathbf{10}}}$	$a$	$b$	$c$	$\delta$	$\theta_N$	$\theta_\Sigma$
1600	1753.3	106.7	146.7	100.1	114.4	$29.0^\circ$	$50.8^\circ$

The equivalence of the two off-diagonal elements can be verified when the symmetry breaking term is given by  $\lambda_8$  due to a finite strange quark mass<sup>26</sup>.

The physical states  $|N_i\rangle$  and  $|\Sigma_i\rangle$  diagonalize  $\mathcal{H}$ . Therefore, we have the relations

$$\tan 2\theta_N = \frac{2\delta}{M_{\overline{\mathbf{10}}} - M_{\mathbf{8}} - a + b - \frac{1}{2}c}, \quad \tan 2\theta_\Sigma = \frac{2\delta}{M_{\overline{\mathbf{10}}} - M_{\mathbf{8}} - 2c}.$$

Now we have the mass formulae for the states

$$\begin{aligned} M_\Theta &= M_{\overline{\mathbf{10}}} - 2a, \\ M_{N_1} &= \left( M_{\mathbf{8}} - b + \frac{1}{2}c \right) \cos^2 \theta_N + (M_{\overline{\mathbf{10}}} - a) \sin^2 \theta_N - \delta \sin 2\theta_N, \\ M_{N_2} &= \left( M_{\mathbf{8}} - b + \frac{1}{2}c \right) \sin^2 \theta_N + (M_{\overline{\mathbf{10}}} - a) \cos^2 \theta_N + \delta \sin 2\theta_N, \\ M_{\Sigma_1} &= (M_{\mathbf{8}} + 2c) \cos^2 \theta_\Sigma + M_{\overline{\mathbf{10}}} \sin^2 \theta_\Sigma - \delta \sin 2\theta_\Sigma, \\ M_{\Sigma_2} &= (M_{\mathbf{8}} + 2c) \sin^2 \theta_\Sigma + M_{\overline{\mathbf{10}}} \cos^2 \theta_\Sigma + \delta \sin 2\theta_\Sigma, \\ M_\Lambda &= M_{\mathbf{8}}, \\ M_{\Xi_8} &= M_{\mathbf{8}} + b + \frac{1}{2}c, \\ M_{\Xi_{\overline{\mathbf{10}}}} &= M_{\overline{\mathbf{10}}} + a. \end{aligned}$$

We have altogether six parameters  $M_{\mathbf{8}}$ ,  $M_{\overline{\mathbf{10}}}$ ,  $a$ ,  $b$ ,  $c$  and  $\delta$  to describe 8 masses. Eliminating the mixing angles and  $\delta$ , we obtain a relation independent of the mixing angle<sup>26</sup>

$$2(M_{N_1} + M_{N_2} + M_{\Xi_8}) = M_{\Sigma_1} + M_{\Sigma_2} + 3M_\Lambda + M_\Theta.$$

Let us first examine the case of  $J^P = 1/2^+$ . Fixing  $\Theta(1540)$ ,  $N_1(1440)$ ,  $N_2(1710)$ ,  $\Lambda(1600)$ ,  $\Sigma_1(1660)$ ,  $\Xi_{\overline{\mathbf{10}}}(1860)$ , we obtain the parameters as given in Table 2. The resulting mass spectrum together with the two predicted masses,  $\Sigma_2 = 1894$  MeV and  $\Xi_8 = 1797$  MeV, are given in Table 3 and also shown in the left panel of Fig. 1. In Fig. 1, the spectra from experiment and those before the representation mixing are also plotted.



Table 3. Mass spectra for  $1/2^+$  case. All values are listed in MeV. Values in parenthesis ( $\Sigma_2$  and  $\Xi_8$ ) are predictions (those which are not used in the fitting).

$\Theta$	$N_1$	$N_2$	$\Sigma_1$	$\Sigma_2$	$\Lambda$	$\Xi_8$	$\Xi_{\overline{10}}$
1540	1440	1710	1660	[1894]	1600	[1797]	1860

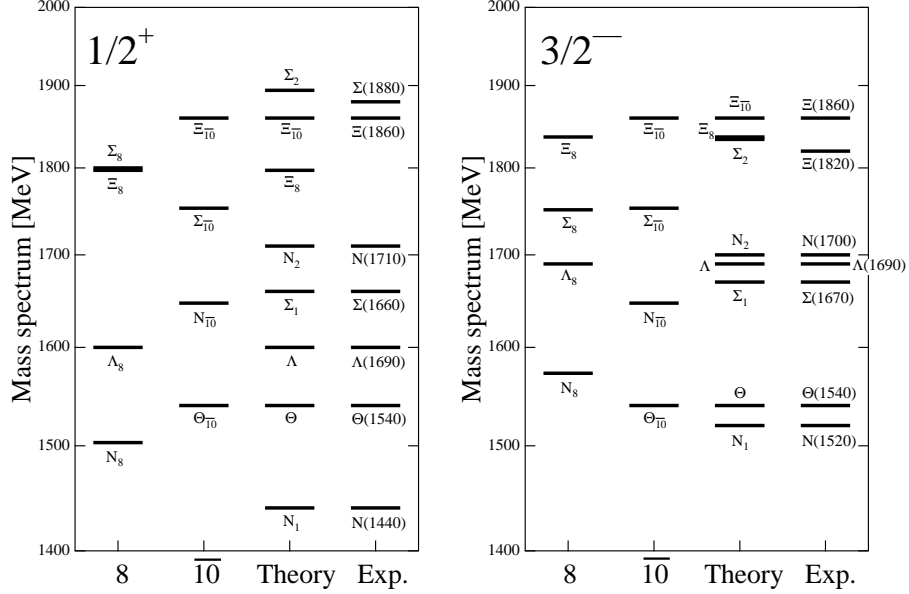


Figure 1. Results of mass spectra with representation mixing. Theoretical masses of the octet, antidecuplet, and the one with mixing are compared with the experimental masses. In the left panel, we show the results with  $J^P = 1/2^+$ , while the results with  $J^P = 3/2^-$  are presented in the right panel.

As we see in Table 3 and Fig. 1, even without using the  $\Sigma_2$  for the fitting, this state appears in the proper position to be assigned as  $\Sigma(1880)$ . Taking into account the experimental uncertainty in the masses, the present result can be regarded as the same as that in Ref. 9, where all known resonances including  $\Sigma(1660)$  and  $\Sigma(1880)$  are used to perform the  $\chi^2$  fitting. In this scheme, we need a new  $\Xi$  state around 1790-1800 MeV to complete the multiplet, but the overall description of the mass spectrum is acceptable. Note that the mixing

Table 4. Parameters for  $3/2^-$  case. All values are listed in MeV except for the mixing angles.

$M_{\mathbf{8}}$	$M_{\overline{\mathbf{10}}}$	$a$	$b$	$c$	$\delta$	$\theta_N$	$\theta_\Sigma$
1690	1753.3	106.7	131.9	30.5	82.2	33.0°	44.6°

angle  $\theta_N \sim 30^\circ$  is compatible with the one of the ideal mixing, if we consider the experimental uncertainty of masses.

It is interesting to observe that in the spectrum of the octet, as shown in Fig. 1, the  $\Xi_8$  and the  $\Sigma_8$  are almost degenerate, reflecting the large value for the parameter  $c \sim 100$  MeV, which is responsible for the splitting of  $\Lambda$  and  $\Sigma$ . For the ground state octet, Eq. (7) is well satisfied with  $b = 139.3$  MeV and  $c = 40.2$  MeV<sup>26</sup>. This point will be discussed later.

Now we examine the other cases of  $J^P$ . For  $J^P = 1/2^-$ , as we observed in the previous section, the pure  $\overline{\mathbf{10}}$  assignment works well for the mass spectrum, which implies that the mixing with  $\mathbf{8}$  is small, as long as we adopt  $N(1650)$  and  $\Sigma(1750)$  in the multiplet. Then the results of  $1/2^-$  with the mixing do not change from the previous results of the pure  $\overline{\mathbf{10}}$  assignment, which eventually lead to a broad width of  $\Theta^+ \rightarrow KN$  of order 100 MeV. Hence, it is not realistic to assign  $1/2^-$ , even if we consider the representation mixing.

Next we consider the  $3/2^+$  case. In this case candidate states are not well established. Furthermore, the states are distributed in a wide energy range, and sometimes it is not possible to assign these particles in the  $\mathbf{8}-\overline{\mathbf{10}}$  representation scheme. Therefore, at this moment, it is not meaningful to study the  $3/2^+$  case unless more states with  $3/2^+$  will be observed.

Now we look at the  $3/2^-$  case. In contrast to the  $3/2^+$  case, there are several well-established resonances. Following the same procedure as before, we first choose the following six resonances as inputs:  $\Theta(1540)$ ,  $N_1(1700)$ ,  $N_2(1520)$ ,  $\Sigma(1670)$ ,  $\Lambda(1690)$ , and  $\Xi_{3/2}(1860)$ . We then obtain the parameters as given in Table 4, and predicted masses of other members are shown in Table 5. The masses of  $N(1520)$  and  $N(1700)$  determine the mixing angle of nucleons  $\theta_N \sim 33^\circ$ , which is close to the ideal one. Interestingly, the fitting provides  $M_{\Xi_8} \sim 1837$  MeV, which is close to the known three-star resonance  $\Xi(1820)$  of  $J^P = 3/2^-$ . We have obtained acceptable assignments, although a new  $\Sigma$  state is necessary to complete the multiplet in both cases. The mass spectrum is also shown in Fig. 1. We have also tried other possible assignments in Ref. 1.

Let us briefly look at the octet and antidecuplet spectra of  $1/2^+$  and  $3/2^-$  resonances as shown in Fig. 1. The antidecuplet spectrum is simple, since the

Table 5. Mass spectra for  $3/2^-$  case. All values are listed in MeV. Values in parenthesis are predictions (those which are not used in the fitting).

$\Theta$	$N_1$	$N_2$	$\Sigma_1$	$\Sigma_2$	$\Lambda$	$\Xi_8$	$\Xi_{\overline{10}}$
1540	1520	1700	1670	[1834]	1690	[1837]	1860

GMO mass formula contains only one parameter which describes the size of the splitting. Contrarily, the octet spectrum contains two parameters which could reflect more information on different internal structure. As mentioned before, in the octet spectrum of  $1/2^+$ , the mass of  $\Sigma_8$  is pushed up slightly above  $\Xi_8$ , significantly higher than  $\Lambda_8$ . This pattern resembles the octet spectrum which is obtained in the Jaffe-Wilczek model, where baryons are made with two flavor  $\mathbf{\overline{3}}$  diquarks and one antiquark. In contrast, the spectrum of the octet of  $3/2^-$  resembles the one of the ground state octet; we find the parameters  $(b, c) = (131.9, 30.5)$  MeV, which are close to  $(b, c) = (139.3, 40.2)$  MeV for the ground states. This is not far from the prediction of an additive quark model of three valence quarks. It would be interesting to investigate further the quark contents from such a different pattern of the mass spectrum.

#### 2.4 Decay width

In the previous subsection, mass spectra of the  $J^P = 1/2^+$  and  $J^P = 3/2^-$  are reasonably well described. Here we study the consistency of the mixing angle obtained from mass spectra with the one obtained from nucleon decay widths for these two cases. Using Eq. (3), we define a universal coupling constant  $g_{\overline{10}}$  as

$$g_{\Theta KN} = \sqrt{6}g_{N_{\overline{10}}\pi N} \equiv g_{\overline{10}}.$$

The coupling constants of the  $\pi N$  decay modes from the  $N_8$ ,  $N_1$ , and  $N_2$  are defined as  $g_{N_8}$ ,  $g_{N_1}$ , and  $g_{N_2}$ , respectively. Under the representation mixing, these constants are related to each other by

$$g_{N_1} = g_{N_8} \cos \theta_N - \frac{g_{\overline{10}}}{\sqrt{6}} \sin \theta_N,$$

$$g_{N_2} = \frac{g_{\overline{10}}}{\sqrt{6}} \cos \theta_N + g_{N_8} \sin \theta_N,$$

and the constants can be translated into the decay widths through Eq. (2). Notice, however, that we cannot fix the relative phase between  $g_{N_8}$  and  $g_{\overline{10}}$ . Hence, there are two possibilities of mixing angles both of which reproduce the same decay widths of  $N_1$  and  $N_2$ .

Table 6. Experimental data for the decay of  $N^*$  resonances. We denote the total decay width and partial decay width to the  $\pi N$  channel as  $\Gamma_{\text{tot}}$  and  $\Gamma_{\pi N}$ , respectively. Values in parenthesis are the central values quoted in PDG<sup>28</sup>.

$J^P$	Resonance	$\Gamma_{\text{tot}}$ [MeV]	Fraction ( $\Gamma_{\pi N}/\Gamma_{\text{tot}}$ )
$1/2^+$	$N(1440)$	250-450 (350)	60-70 (65) %
	$N(1710)$	50-250 (100)	10-20 (15) %
$3/2^-$	$N(1520)$	110-135 (120)	50-60 (55) %
	$N(1700)$	50-150 (100)	5-15 (10) %

Table 7. Decay width of  $\Theta^+$  determined from the nucleon decays and the mixing angle obtained from the mass spectra. Phase 1 corresponds to the same signs of  $g_{N\mathbf{8}}$  and  $g_{\overline{\mathbf{10}}}$ , while phase 2 corresponds to the opposite signs. All values are listed in MeV.

$J^P$	$\theta_N$	$\Gamma_\Theta$ (Phase 1)	$\Gamma_\Theta$ (Phase 2)
$1/2^+$	$29^\circ$ (Mass)	29.1	103.3
$3/2^-$	$33^\circ$ (Mass)	3.1	20.0

For  $J^P = 1/2^+$  and  $3/2^-$ , we display the decay widths and branching ratios to the  $\pi N$  channel of relevant nucleon resonances in Table 6. Using the mixing angle determined from the mass spectrum and experimental information of  $N^* \rightarrow \pi N$  decays, we obtain the decay width of the  $\Theta^+$  as shown in Table 7. Among the two values, the former corresponds to the same signs of  $g_{N\mathbf{8}}$  and  $g_{\overline{\mathbf{10}}}$  (phase 1), while the latter to the opposite signs (phase 2).

Let us adopt the narrower results of phase 1. For the  $1/2^+$  case, the width is about 30 MeV, which exceeds the upper bound of the experimentally observed width. In contrast, the  $3/2^-$  case predicts much narrower width of the order of a few MeV, which is compatible with the experimental upper bound of the  $\Theta^+$  width. Considering the agreement of mixing angles and the relatively small uncertainties in the experimental decay widths, the results with the  $3/2^-$  case are favorable in the present fitting analysis.

### 3 Two-meson coupling and reaction processes

We have performed a phenomenological analysis on the exotic particles using flavor SU(3) symmetry. Let us briefly summarize what we have done. It is found that the masses of  $\Theta(1540)$  and  $\Xi_{3/2}(1860)$  are well fitted into an antidecuplet ( $\overline{\mathbf{10}}$ ) representation which mixes with an octet ( $\mathbf{8}$ ), with known baryon resonances of  $J^P = 1/2^+$  or  $3/2^-$ . Under the representation mixing,

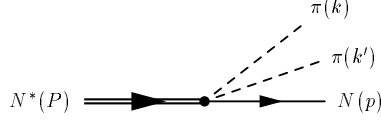


Figure 2. Feynman diagram for the three-body decay of the  $N^*$  resonance.

Table 8. Experimental information of two-pion decay of nucleon resonances. “Scalar” represents the mode  $\pi\pi(I=0, s \text{ wave})N$  and “Vector” means  $\pi\pi(I=1, p \text{ wave})N$  mode. Values in parenthesis are averaged over the interval quoted in PDG<sup>28</sup>.

$J^P$	State	$\Gamma_{\text{tot}}$ [MeV]	Scalar [%]	Vector [%]
$1/2^+$	$N(1440)$	350	5-10(7.5)	<8
	$N(1710)$	100	10-40(25)	5-25(15)
$3/2^-$	$N(1520)$	120	10-40(25)	15-25(20)
	$N(1700)$	100	< 85-95	<35

the physical nucleon states are defined as Eq. (4). Two states  $N_1$  and  $N_2$  represent  $N(1440)$  and  $N(1710)$  for the  $1/2^+$  case, while  $N(1520)$  and  $N(1700)$  for the  $3/2^-$  case. The mixing angles  $\theta_N$  are determined by experimental spectra of known resonances as  $\theta_N = 29^\circ$  for  $J^P = 1/2^+$  and  $\theta_N = 33^\circ$  for  $J^P = 3/2^-$ , as shown in Tables 2 and 4. Using these mixing angles and decay widths of nucleon resonances ( $\Gamma_{N^* \rightarrow \pi N}$ ), we calculate the decay width of  $\Theta$  ( $\Gamma_{\Theta \rightarrow KN}$ ) through the SU(3) relation between the coupling constants. Here we examine the phenomenology of three-body decays, as shown in Fig. 2.

In Table 8, we show the experimental information of the decay pattern of the nucleon resonances  $N^* \rightarrow \pi\pi N$  taken from PDG<sup>28</sup>. For convenience, we refer to  $\pi\pi(I=0, s \text{ wave})N$  and  $\pi\pi(I=1, p \text{ wave})N$  modes as “scalar” ( $s$ ) and “vector” ( $v$ ), respectively. We adopt the total branching ratio to  $\pi\pi N$  channel as the upper limit of the branch for  $\pi\pi(I=0)N$  state,  $BR_{N(1700) \rightarrow \pi\pi(I=0)N} < 85\text{-}95\%$ , since there is no information for the scalar decay of  $N(1700)$ .

### 3.1 Effective interaction Lagrangians

Here we write down the effective Lagrangians that account for the relevant interactions in the present analysis. We need two steps, namely, the extraction of the  $\overline{\mathbf{10}}$  component from the  $N^* \rightarrow \pi\pi N$  decay and the extrapolation of that term to the  $\Theta\pi KN$  channel. Lagrangians for nucleons will be used for the

former purpose; the Lagrangians for the antidecuplet will tell us the SU(3) relation among different channels in the multiplet.

Using the partial decay widths of the two nucleon resonances  $\Gamma_i^{s,v}$ , we determine the absolute values of the coupling constants  $|g_i^{s,v}|$ , where superscripts  $s$  and  $v$  stand for the scalar- and vector-type correlations of two mesons. From them, we can obtain the antidecuplet and octet components of the  $N^*\pi\pi N$  coupling constants as

$$\begin{aligned} g^{s,v}(\overline{\mathbf{10}}) &= -|g_1^{s,v}| \sin \theta_N \pm |g_2^{s,v}| \cos \theta_N, \\ g^{s,v}(\mathbf{8}) &= |g_1^{s,v}| \cos \theta_N \pm |g_2^{s,v}| \sin \theta_N, \end{aligned} \quad (8)$$

based on Eq. (4). Here we use  $\theta_N$  obtained from the mass spectra. We include experimental uncertainties of the  $N^*$  decays, which will be reflected in uncertainties of  $g^{s,v}(\overline{\mathbf{10}})$ .

To write down the interaction Lagrangians, we adopt the following conventions for the fields (nucleons  $N$ , nucleon resonances  $N^*$ , pions  $\pi$ , octet meson  $\phi$ , octet baryon  $B$  and antidecuplet baryon  $P$ ) :

$$N = \begin{pmatrix} p \\ n \end{pmatrix}, \quad N_i^* = \begin{pmatrix} p_i^* \\ n_i^* \end{pmatrix}, \quad \pi = \begin{pmatrix} \pi^0 & \sqrt{2}\pi^+ \\ \sqrt{2}\pi^- & -\pi^0 \end{pmatrix},$$

$$\begin{aligned} \phi &= \begin{pmatrix} \frac{1}{\sqrt{2}}\pi^0 + \frac{1}{\sqrt{6}}\eta & \pi^+ & K^+ \\ \pi^- & -\frac{1}{\sqrt{2}}\pi^0 + \frac{1}{\sqrt{6}}\eta & K^0 \\ K^- & \bar{K}^0 & -\frac{2}{\sqrt{6}}\eta \end{pmatrix}, \\ B &= \begin{pmatrix} \frac{1}{\sqrt{2}}\Sigma^0 + \frac{1}{\sqrt{6}}\Lambda & \Sigma^+ & p \\ \Sigma^- & -\frac{1}{\sqrt{2}}\Sigma^0 + \frac{1}{\sqrt{6}}\Lambda & n \\ \Xi^- & \Xi^0 & -\frac{2}{\sqrt{6}}\Lambda \end{pmatrix}, \end{aligned}$$

$$\begin{aligned} P^{333} &= \sqrt{6}\Theta_{10}^+, & P^{133} &= \sqrt{2}N_{10}^0, & P^{233} &= -\sqrt{2}N_{10}^+, \\ P^{113} &= \sqrt{2}\Sigma_{10}^-, & P^{123} &= -\Sigma_{10}^0, & P^{223} &= -\sqrt{2}\Sigma_{10}^+, \\ P^{111} &= \sqrt{6}\Xi_{10}^{--}, & P^{112} &= -\sqrt{2}\Xi_{10}^-, & P^{122} &= \sqrt{2}\Xi_{10}^0, \\ P^{222} &= -\sqrt{6}\Xi_{10}^+. \end{aligned}$$

The interaction Lagrangians for nucleons with  $J^P = 1/2^+$  are

$$\begin{aligned} \mathcal{L}_i^s &= \frac{g_i^s}{2\sqrt{2}f} \bar{N}_i^* \pi \cdot \pi N + \text{h.c.} \\ \mathcal{L}_i^v &= i \frac{g_i^v}{4\sqrt{2}f^2} \bar{N}_i^* (\pi \cdot \not{\partial} \pi - \not{\partial} \pi \cdot \pi) N + \text{h.c.}, \end{aligned}$$

where  $f = 93$  MeV is the pion decay constant,  $g_i^{s,v}$  are dimensionless coupling constants, and h.c. stands for the hermitian conjugate. Subscript  $i = 1, 2$  denotes the two nucleons  $N(1440)$  and  $N(1710)$ , respectively. The interaction Lagrangian for the antidecuplet can be written as

$$\begin{aligned}\mathcal{L}_{1/2^+}^s &= \frac{g_{1/2^+}^s}{2f} \bar{P}_{ijk} \epsilon^{lmk} \phi_l^a \phi_a^i B_m^j + \text{h.c.}, \\ \mathcal{L}_{1/2^+}^v &= i \frac{g_{1/2^+}^v}{4f^2} \bar{P}_{ijk} \epsilon^{lmk} \gamma^\mu (\partial_\mu \phi_l^a \phi_a^i - \phi_l^a \partial_\mu \phi_a^i) B_m^j + \text{h.c.}\end{aligned}$$

with the coupling constants for the antidecuplet baryon  $g_{1/2^+}^s, g_{1/2^+}^v$ .

In the same way, the Lagrangians for the  $J^P = 3/2^-$  case can be written. We express the spin 3/2 baryons as Rarita-Schwinger fields  $B^{\mu 29}$ . The effective Lagrangians for nucleons are given by

$$\begin{aligned}\mathcal{L}_i^s &= i \frac{g_i^s}{4\sqrt{2}f^2} \bar{N}_i^{*\mu} \partial_\mu (\boldsymbol{\pi} \cdot \boldsymbol{\pi}) N + \text{h.c.} \\ \mathcal{L}_i^v &= i \frac{g_i^v}{4\sqrt{2}f^2} \bar{N}_i^{*\mu} (\boldsymbol{\pi} \cdot \partial_\mu \boldsymbol{\pi} - \partial_\mu \boldsymbol{\pi} \cdot \boldsymbol{\pi}) N + \text{h.c.}\end{aligned}$$

Here  $i = 1, 2$  denotes the two nucleons  $N(1520)$  and  $N(1700)$ , respectively. The Lagrangians for the antidecuplet are constructed as a straightforward extension of those for  $1/2^+$  case:

$$\begin{aligned}\mathcal{L}_{3/2^-}^s &= i \frac{g_{3/2^-}^s}{4f^2} \bar{P}_{ijk}^\mu \epsilon^{lmk} \partial_\mu (\phi_l^a \phi_a^i) B_m^j + \text{h.c.} \\ \mathcal{L}_{3/2^-}^v &= i \frac{g_{3/2^-}^v}{4f^2} \bar{P}_{ijk}^\mu \epsilon^{lmk} (\partial_\mu \phi_l^a \phi_a^i - \phi_l^a \partial_\mu \phi_a^i) B_m^j + \text{h.c.}\end{aligned}$$

### 3.2 Evaluation of the coupling constants

To study the coupling constants, let us start with the decay width of a resonance into two mesons and one baryon, which is given by

$$\Gamma_{N\pi\pi} = \frac{M}{16\pi^3} \int_{\omega_{\min}}^{\omega_{\max}} d\omega \int_{\omega'_{\min}}^{\omega'_{\max}} d\omega' \bar{\Sigma} \Sigma |t(\omega, \omega', a)|^2 \Theta(1 - a^2),$$

with

$$\begin{aligned}\omega_{\min} = \omega'_{\min} &= m, \quad \omega_{\max} = \omega'_{\max} = \frac{M_R^2 - M^2 - 2Mm}{2M_R}, \\ a = \cos \theta &= \frac{(M_R - \omega - \omega')^2 - M^2 - |\mathbf{k}|^2 - |\mathbf{k}'|^2}{2|\mathbf{k}||\mathbf{k}'|},\end{aligned}$$

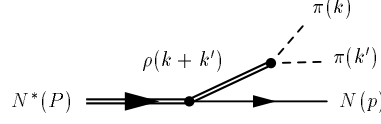


Figure 3. Three-body decay of the  $N^*$  resonance with insertion of the vector meson propagator.

where we assign the momentum variables  $P = (M_R, \mathbf{0})$ ,  $k = (\omega, \mathbf{k})$ ,  $k' = (\omega', \mathbf{k}')$ , and  $p = (E, \mathbf{p})$  as in Fig. 2.  $M_R$ ,  $M$ , and  $m$  are the masses of the resonance, baryon, and mesons, respectively, and  $\theta$  is the angle between the momenta  $\mathbf{k}$  and  $\mathbf{k}'$ . The on-shell energies of particles are given by  $\omega = \sqrt{m^2 + \mathbf{k}^2}$ ,  $\omega' = \sqrt{m^2 + (\mathbf{k}')^2}$ , and  $E = \sqrt{M^2 + \mathbf{p}^2}$ ;  $\Theta$  denotes the step function; and  $\bar{\Sigma}\Sigma$  stands for the spin sum of the fermion states.

In the following, we evaluate the squared amplitude  $\bar{\Sigma}\Sigma|t(\omega, \omega', \cos \theta)|^2$  for the  $N^* \rightarrow \pi\pi N$  decay in the nonrelativistic approximation. For  $J^P = 1/2^+$ ,

$$\begin{aligned} \bar{\Sigma}\Sigma|t_{1/2^+}^s|^2 &= 3 \left( \frac{g_{1/2^+}^s}{2f} \right)^2 \frac{E + M}{2M}. \\ \bar{\Sigma}\Sigma|t_{1/2^+}^v|^2 &= 6 \left( \frac{g_{1/2^+}^v}{4f^2} \right)^2 \frac{1}{2M} \left\{ (E + M)(\omega - \omega')^2 + 2(|\mathbf{k}|^2 - |\mathbf{k}'|^2)(\omega - \omega') \right. \\ &\quad \left. + (E - M)(\mathbf{k} - \mathbf{k}')^2 \right\} \times \left| \frac{-m_\rho^2}{s' - m_\rho^2 + im_\rho\Gamma(s')} \right|^2. \end{aligned}$$

For the vector-type coupling, we have inserted the vector meson propagator to account for the  $\rho$  meson correlation<sup>13</sup>, as shown in Fig. 3.  $m_\rho$  is the mass of  $\rho$  meson,  $s' = (k + k')^2$ .  $\Gamma(s')$  is the energy-dependent width given by

$$\Gamma(s') = \Gamma_\rho \times \left( \frac{p_{\text{cm}}(s')}{p_{\text{cm}}(m_\rho^2)} \right)^3,$$

where  $p_{\text{cm}}(s')$  is the relative three-momentum of the final two particles in the  $\rho$  rest frame. For  $J^P = 3/2^-$ , we have

$$\begin{aligned} \bar{\Sigma}\Sigma|t_{3/2^-}^s|^2 &= \left( \frac{g_{3/2^-}^s}{4f^2} \right)^2 (\mathbf{k} + \mathbf{k}')^2 \frac{E + M}{2M}, \\ \bar{\Sigma}\Sigma|t_{3/2^-}^v|^2 &= 2 \left( \frac{g_{3/2^-}^v}{4f^2} \right)^2 (\mathbf{k} - \mathbf{k}')^2 \frac{E + M}{2M} \left| \frac{-m_\rho^2}{s' - m_\rho^2 + im_\rho\Gamma(s')} \right|^2. \end{aligned}$$



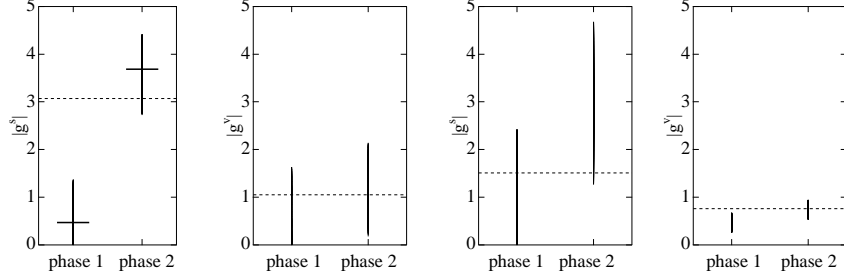


Figure 4. Numerical results for the coupling constants with  $J^P = 1/2^+$  (Left two panels) and with  $3/2^-$  (Right two panels). The two choices of the relative phase between coupling constants are marked as “phase 1” and “phase 2”. Allowed regions of the coupling constants are shown by the vertical bar. Horizontal bars represent the results obtained with the averaged values, which are absent for the vector case. Horizontal dashed lines show the upper limits of the coupling constants derived from the self-energy  $|\text{Re}\Sigma| < 200$  MeV.

Now we evaluate the coupling constants numerically. Using the averaged values in Table 8, we obtain the coupling constants  $g_i^s$  and  $g_i^v$  for these channels. By substituting them into Eq. (8) (but suppressing the label  $\overline{10}$  for simplicity), the antidecuplet components are extracted as

$$|g_{1/2^+}^s| = 0.47, \quad 3.68, \quad (9)$$

where two values correspond to the results with different relative phases between the two coupling constants. When we take into account the experimental uncertainties in branching ratio, the antidecuplet components can vary within the following ranges:

$$0 < |g_{1/2^+}^s| < 1.37, \quad 0 < |g_{1/2^+}^v| < 2.14, \\ 2.72 < |g_{1/2^+}^s| < 4.42,$$

including the two cases of different phase. These uncertainties are also shown by the vertical bars in Fig. 4, with the horizontal bars being the result with the averaged value in Eq. (9).

Let us consider phenomenological implications of this result. In Ref. 13, we evaluated the self-energy of the baryon antidecuplet due to two-meson coupling. The coupling constants was derived by assuming that the  $\Theta^+$  belongs to a pure antidecuplet together with  $N(1710)$ , where we determined  $|g_{1/2^+}^s| = 1.88$  and  $|g_{1/2^+}^v| = 0.315$ . In the calculation of the self-energy of  $\Theta^+$ , the effect of the mixing only changes the coupling constants, by neglecting the small contribution from  $\mathcal{L}^{27}$ . In this case, the  $\Theta^+$  self-energy with the

new coupling constants can be obtained by simple rescaling. Using the values of Eq. (9), we estimate

$$\Sigma_{\Theta^+}^s = -287, \quad -4.7 \text{ MeV}, \quad 0 > \Sigma_{\Theta^+}^v > -770 \text{ MeV}.$$

The sum of these values are the contribution to the self-energy of  $\Theta^+$  from the two-meson cloud. Naively, we expect that it should be of the order of 100 MeV, at most  $\sim 20\%$  of the total energy<sup>13</sup>. From this consideration, we adopt the condition that the magnitude of one of the contributions should not exceed 200 MeV:  $|\text{Re}\Sigma_{\Theta^+}| < 200$ . This condition is satisfied when

$$|g_{1/2^+}^s| < 3.07, \quad |g_{1/2^+}^v| < 1.05. \quad (10)$$

Therefore, we can exclude the choice of “phase 2” in left two panels in Fig. 4. The limit for  $|g_{1/2^+}^v|$  is compatible with Eq. (9), although the self-energy argument gives a more stringent constraint. These upper limits are also shown in Fig. 4 by the dashed lines.

Now we consider the  $J^P = 3/2^-$  case. Using the central values in Table 8, we obtain the coupling constants  $g_i^s$  and  $g_i^v$  for these channels. In this case, with the same reason as in the vector coupling for the  $1/2^+$  case, the central value cannot be determined. Experimental uncertainties allows the antidecuplet components to vary within the following ranges:

$$0 < |g_{3/2^-}^s| < 4.68, \quad 0.25 < |g_{3/2^-}^v| < 0.94,$$

including the two cases of different phase. The results are shown by the vertical bars in right two panels of Fig. 4.

We can also estimate the magnitude of the self-energy, by substituting the squared amplitudes for  $3/2^-$  case in the formulas of the self-energy shown in Ref. 13. For instance, we estimate the real part of the self-energy as  $-1518$  MeV for an initial energy of 1540-1700 MeV and a cutoff of 700-800 MeV for  $|g_{3/2^-}^s| = 4.17$ . The huge self-energy is due to the  $p$ -wave nature of the two-meson coupling. In this way, to have some reasonable values for the self-energy  $|\text{Re}\Sigma_{\Theta^+}| < 200$  MeV,

$$|g_{3/2^-}^s| < 1.51, \quad |g_{3/2^-}^v| < 0.76.$$

Both upper limits are indicated by horizontal dashed lines in the right two panels in Fig. 4.

### 3.3 Analysis of the meson-induced reactions

As an application of effective Lagrangians, we calculate the reaction processes  $\pi^- p \rightarrow K^- \Theta^+$  and  $K^+ p \rightarrow \pi^+ \Theta^+$  via tree-level diagrams as shown in

Fig. 5. These are alternative reactions to, for instance, photo-induced reactions, which are useful for further study of the  $\Theta^+$ . The amplitudes for these reactions are given by

$$\begin{aligned} -it_{1/2+}^s(\pi^- p \rightarrow K^- \Theta^+) &= -it_{1/2+}^s(K^+ p \rightarrow \pi^+ \Theta^+) \\ &= i \frac{g_{1/2+}^s}{2f} (-\sqrt{6}) N_{\Theta^+} N_p, \end{aligned} \quad (11)$$

$$\begin{aligned} -it_{1/2+}^v(\pi^- p \rightarrow K^- \Theta^+) &= it_{1/2+}^v(K^+ p \rightarrow \pi^+ \Theta^+) \\ &= i \frac{g_{1/2+}^v}{4f^2} (-\sqrt{6}) (2\sqrt{s} - M_{\Theta} - M_p) N_{\Theta^+} N_p F(k - k') \end{aligned} \quad (12)$$

for the  $1/2^+$  case and by

$$\begin{aligned} -it_{3/2-}^s(\pi^- p \rightarrow K^- \Theta^+) &= -it_{3/2-}^s(K^+ p \rightarrow \pi^+ \Theta^+) \\ &= i \frac{g_{3/2-}^s}{4f^2} (-\sqrt{6}) (\mathbf{k} - \mathbf{k}') \cdot \mathbf{S}^\dagger N_{\Theta^+} N_p, \\ -it_{3/2-}^v(\pi^- p \rightarrow K^- \Theta^+) &= it_{3/2-}^v(K^+ p \rightarrow \pi^+ \Theta^+) \\ &= -i \frac{g_{3/2-}^v}{4f^2} (-\sqrt{6}) (\mathbf{k} + \mathbf{k}') \cdot \mathbf{S}^\dagger N_{\Theta^+} N_p F(k - k') \end{aligned} \quad (13)$$

for the  $3/2^-$  case, where the normalization factor is  $N_i = \sqrt{(E_i + M_i)/2M_i}$ ,  $\mathbf{S}$  is the spin transition operator,  $\sqrt{s}$  is the initial energy, and  $k$  and  $k'$  are the momenta of the incoming and outgoing mesons, respectively. Here we define the vector meson propagator (Fig. 5, right) as

$$F(k - k') = \frac{-m_{K^*}^2}{(k - k')^2 - m_{K^*}^2 + im_{K^*} \Gamma[(k - k')^2]}, \quad (14)$$

which is included in the vector-type amplitude. In the kinematical region in which we are interested, the momentum-dependent decay width of  $K^*$ ,  $\Gamma[(k - k')^2]$  vanishes.

Since the two amplitudes must be summed coherently, the squared am-

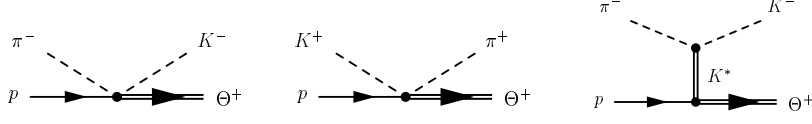


Figure 5. Feynman diagrams for the meson-induced reactions for  $\Theta^+$  production. Right :  $\pi^- p \rightarrow K^- \Theta^+$  reaction. Center :  $K^+ p \rightarrow \pi^+ \Theta^+$  reaction. Left :  $\pi^- p \rightarrow K^- \Theta^+$  reaction with a vector meson propagator.

plitudes are given by

$$\begin{aligned}
 \bar{\Sigma} \Sigma |t_{1/2+}|^2 &= 6 \left( \frac{1}{2f} \right)^2 N_{\Theta^+}^2 N_p^2 \left[ (g_{1/2+}^s)^2 \right. \\
 &\quad \pm 2g_{1/2+}^s g_{1/2+}^v \frac{2\sqrt{s} - M_{\Theta} - M_p}{2f} F(k - k') \\
 &\quad \left. + (g_{1/2+}^v)^2 \frac{(2\sqrt{s} - M_{\Theta} - M_p)^2}{4f^2} F^2(k - k') \right], \\
 \bar{\Sigma} \Sigma |t_{3/2-}|^2 &= 4 \left( \frac{1}{4f^2} \right)^2 N_{\Theta^+}^2 N_p^2 \left[ (g_{3/2-}^s)^2 (\mathbf{k} - \mathbf{k}')^2 \right. \\
 &\quad \mp 2g_{3/2-}^s g_{3/2-}^v (|\mathbf{k}|^2 - |\mathbf{k}'|^2) F(k - k') \\
 &\quad \left. + (g_{3/2-}^v)^2 (\mathbf{k} + \mathbf{k}')^2 F^2(k - k') \right],
 \end{aligned} \tag{15}$$

where  $\pm$  and  $\mp$  signs denote the  $\pi^- p \rightarrow K^- \Theta^+$  and  $K^+ p \rightarrow \pi^+ \Theta^+$  reactions, respectively. Notice that the relative phase between the two coupling constants is important, which affects the interference term of the two amplitudes. To determine the phase, we use the experimental information from  $\pi^- p \rightarrow K^- \Theta^+$  reaction at KEK<sup>31,24</sup>, where the upper limit of the cross section has been extracted to be a few  $\mu\text{b}$ .

The differential cross section for these reactions is given by

$$\frac{d\sigma}{d\cos\theta}(\sqrt{s}, \cos\theta) = \frac{1}{4\pi s} \frac{|\mathbf{k}'|}{|\mathbf{k}|} M_p M_{\Theta} \frac{1}{2} \bar{\Sigma} \Sigma |t(\sqrt{s}, \cos\theta)|^2,$$

which is evaluated in the center-of-mass frame. The total cross section can be obtained by integrating this over  $\cos\theta$ .

### 3.4 Qualitative features of the cross sections

Now let us calculate the cross section using the coupling constants obtained previously. Here we focus on the qualitative difference between  $J^P = 1/2^+$

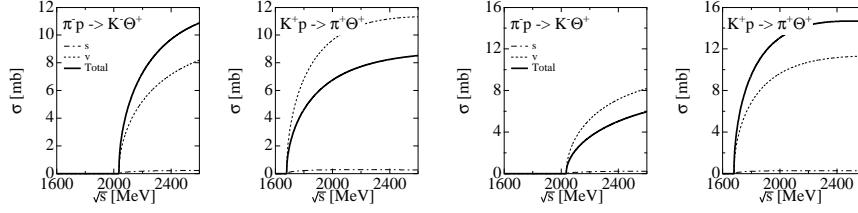


Figure 6. Total cross sections for the  $J^P = 1/2^+$  case with  $g^s = 0.47$  and  $g^v = 0.47$  (Left two panels) and with  $g^v = -0.47$  (Right two panels). The thick line shows the result with full amplitude. Dash-dotted and dashed lines are the contributions from  $s$  and  $v$  terms, respectively.

and  $3/2^-$  cases. We first calculate for the  $1/2^+$  case, with coupling constants

$$g_{1/2^+}^s = 0.47, \quad g_{1/2^+}^v = 0.47, \quad (16)$$

where  $g_{1/2^+}^s$  is one of the solutions that satisfies the condition (10). Since the result for  $g_{1/2^+}^v$  spreads over a wide range, we choose  $g_{1/2^+}^v = g_{1/2^+}^s$ , which is well within the allowed region determined from the self-energy. The result is shown in the left two panels in Fig. 6, with individual contributions from  $s$  and  $v$  terms. As we see, the use of the same coupling constant for both terms results in the dominance of the vector term. However, there is a sizable interference effect between  $s$  and  $v$  terms, although the contribution from the  $s$  term itself is small. The two amplitudes interfere constructively for the  $\pi^- p \rightarrow K^- \Theta^+$  channel, whereas in the  $K^+ p \rightarrow \pi^+ \Theta^+$  case they destructively interfere.

As already mentioned, the relative phase of the two coupling constants is not determined. If we change the sign,

$$g_{1/2^+}^s = 0.47, \quad g_{1/2^+}^v = -0.47, \quad (17)$$

then the results change as in the right two panels in Fig. 6, where constructive and destructive interference appears in an opposite manner.

There is an experimental result from KEK<sup>24</sup> that the cross section of  $\pi^- p \rightarrow K^- \Theta^+$  was found to be very small, of the order of a few  $\mu\text{b}$ . This is an order smaller than the typical background processes of this energy, which are of the order of  $30 \mu\text{b}$ <sup>24</sup>. At this stage, we do not want to calculate the cross section quantitatively, but the experimental result suggests that the choice of Eq. (17) should be plausible, for the small cross section of the  $\pi^- p \rightarrow K^- \Theta^+$  reaction. In this case, the cross section for  $K^+ p \rightarrow \pi^+ \Theta^+$  becomes large.

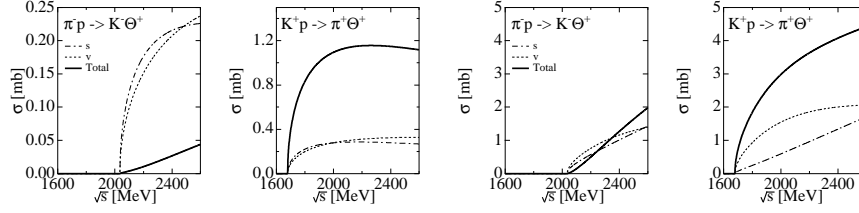


Figure 7. Total cross sections for the  $J^P = 1/2^+$  case with  $g^s = 0.47$  and  $g^v = -0.08$  (Left two panels), and for the  $J^P = 3/2^-$  case with  $g^s = 0.2$  and  $g^v = 0.4$  (Right two panels), when the most destructive interference for  $\pi^- p \rightarrow K^- \Theta^+$  takes place. Note that the vertical scale is different in the two panels. The thick line shows the result with full amplitude. Dash-dotted and dashed lines are the contributions from  $s$  and  $v$  terms, respectively.

As a trial, let us search for the set of coupling constants with which the most destructive interference takes place in  $\pi^- p \rightarrow K^- \Theta^+$ , by changing  $g_{1/2^+}^v$  within the allowed region. This means that the difference between cross sections of  $\pi^- p \rightarrow K^- \Theta^+$  and  $K^+ p \rightarrow \pi^+ \Theta^+$  is maximal. Then we find

$$g_{1/2^+}^s = 0.47, \quad g_{1/2^+}^v = -0.08. \quad (18)$$

The result is shown in left two panels in Fig. 7. A huge difference between  $\pi^- p \rightarrow K^- \Theta^+$  and  $K^+ p \rightarrow \pi^+ \Theta^+$  can be seen. In this case, we observe the ratio of cross sections

$$\frac{\sigma(K^+ p \rightarrow \pi^+ \Theta^+)}{\sigma(\pi^- p \rightarrow K^- \Theta^+)} \sim 50,$$

where we estimated the cross section  $\sigma$  as the average of the cross section shown in the figures (from threshold to 2.6 GeV). Notice that the ratio of the coupling constants  $g_{1/2^+}^s / g_{1/2^+}^v \sim -5.9$  is relevant for the interference effect. It is possible to scale both coupling constants within experimental uncertainties. This does not change the ratio of cross sections, but it does change the absolute values.

Next we examine the case with  $J^P = 3/2^-$ . Again, we observe constructive and destructive interferences, depending on the relative sign of the two amplitudes. The interference effect is prominent around the energy region close to the threshold but is not very strong in the higher energy region, compared with  $1/2^+$  case. We search for the coupling constants with which the most destructive interference takes place for  $\pi^- p \rightarrow K^- \Theta^+$ . We find that destructive interference is maximized when the ratio of the coupling constants

is  $g_{3/2-}^s/g_{3/2-}^v \sim 0.5$ . Taking, for instance, the values

$$g_{3/2-}^s = 0.2, \quad g_{3/2-}^v = 0.4, \quad (19)$$

which are within the experimental bounds, we obtain the results shown in right two panels in Fig. 7. In contrast to the  $J^P = 1/2^+$  case, here the ratio of cross section is not very large:

$$\frac{\sigma(K^+p \rightarrow \pi^+\Theta^+)}{\sigma(\pi^-p \rightarrow K^-\Theta^+)} \sim 3.3.$$

The high-energy behavior in this case is understood from the  $p$ -wave nature of the coupling.

### 3.5 Quantitative analysis

Here we consider the reaction mechanism in detail to provide a more quantitative result. First we introduce a hadronic form factor at the vertices, which accounts for the energy dependence of the coupling constants. Physically, it is understood as the reflection of the finite size of the hadrons. In practice, however, the introduction of the form factor has some ambiguities in its form and the cutoff parameters<sup>30</sup>.

In Ref. 23, the  $\pi^-p \rightarrow K^-\Theta^+$  reaction is studied with a three-dimensional monopole-type form factor

$$F(\sqrt{s}) = \frac{\Lambda^2}{\Lambda^2 + \mathbf{q}^2}, \quad (20)$$

where  $\mathbf{q}^2 = \lambda(s, M_N^2, m_{\text{in}}^2)/4s$  with  $m_{\text{in}}$  being the mass of the incoming meson and  $\Lambda = 0.5$  GeV. Here we adopt this form factor and apply it to the present process. We obtain the results for  $J^P = 1/2^+$  and for  $J^P = 3/2^-$  in left two panels and right two panels in Fig. 8, with the coupling constants given in Eqs. (18) and (19).

We observe that the cross section is suppressed down to  $\sim 1\mu\text{b}$  for the  $\pi^-p \rightarrow K^-\Theta^+$  reaction in the  $1/2^+$  case. However, this is also a consequence of our choice of small coupling constants. Indeed, with these coupling constants, the self-energy of  $\Theta^+$  becomes

$$\text{Re}\Sigma_{\Theta^+}^{1/2^+} = \text{Re}\Sigma_{\Theta^+}^s + \text{Re}\Sigma_{\Theta^+}^v \sim -5.3 - 1.6 = -6.9 \text{ MeV},$$

for  $p^0 = 1700$  MeV and a cutoff 750 MeV. This is too small, but as we mentioned before, we can scale these constants without changing the ratio of  $K^+p \rightarrow \pi^+\Theta^+$  and  $\pi^-p \rightarrow K^-\Theta^+$ . We would like to search for the coupling constants which provide a small cross section for  $\pi^-p \rightarrow K^-\Theta^+$  reaction

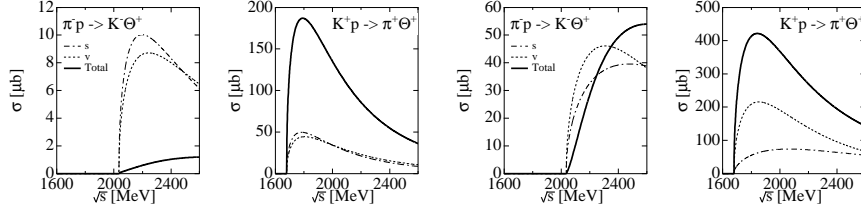


Figure 8. Total cross sections for the  $J^P = 1/2^+$  case with  $g^s = 0.47$  and  $g^v = -0.08$  (Left two panels), and for the  $J^P = 3/2^-$  case with  $g^s = 0.2$  and  $g^v = 0.4$  including a hadronic form factor (20). The thick line shows the result with full amplitude. Dash-dotted and dashed lines are the contributions from  $s$  and  $v$  terms, respectively.

compatible with experiment and a moderate amount of self-energy, which guarantee the dominance of the two-meson coupling terms compared with the  $KN\Theta^+$  vertex.

In Fig. 9, we plot the cross section of  $\pi^- p \rightarrow K^- \Theta^+$  reaction and the self-energy of  $\Theta^+$  by fixing the ratio of coupling constants. The cross section is the value at  $\sqrt{s} = 2124$  MeV, which corresponds to the KEK experiment  $P_{\text{lab}} \sim 1920$  MeV. The horizontal axis denotes the factor  $F$ , which is defined by

$$g_{1/2+}^s = F \times 0.47, \quad g_{1/2+}^v = -F \times 0.08. \quad (21)$$

We use  $F = 1$  for the calculation of Fig. 8. Both the cross section and self-energy are proportional to the square of the coupling constant. By vertical bars, we indicate the points where

- cross section  $\sim 4.1\mu\text{b}^a$  estimated by KEK experiment<sup>31,24</sup>
- upper limit of  $g_{1/2+}^s$
- $\text{Re}\Sigma_{\Theta} = -100$  MeV

For the  $J^P = 3/2^-$  case, with  $g_{3/2-}^s = 0.2$  and  $g_{3/2-}^v = 0.4$ , the self-energy of  $\Theta^+$  becomes

$$\text{Re}\Sigma_{\Theta^+}^{3/2-} = \text{Re}\Sigma_{\Theta^+}^s + \text{Re}\Sigma_{\Theta^+}^v \sim -4 - 80 = -84 \text{ MeV}.$$

In Fig. 9, we plot the cross section of the  $\pi^- p \rightarrow K^- \Theta^+$  reaction and the self-energy of  $\Theta^+$  by fixing the ratio of coupling constants. The horizontal

<sup>a</sup>Here we use the preliminary value  $4.1\mu\text{b}$  reported in Ref. 31, which has been later corrected as  $3.9\mu\text{b}$ <sup>24</sup>. Qualitative conclusions remain unchanged for the upper limit of  $3.9\mu\text{b}$ .



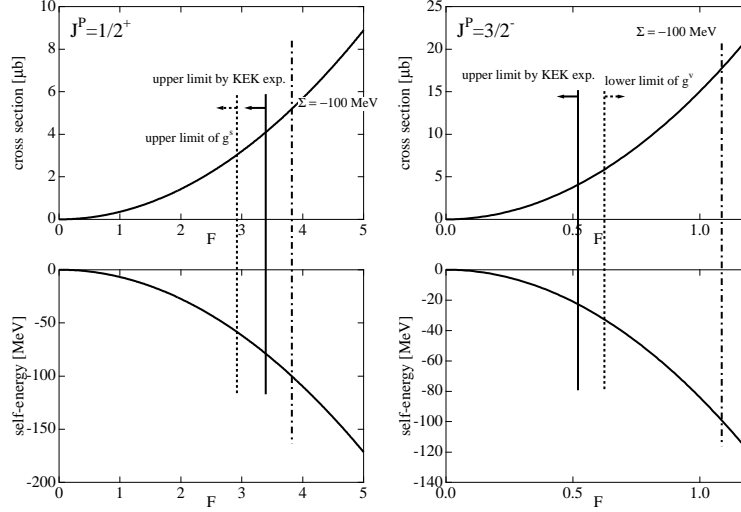


Figure 9. The total cross section of  $\pi^- p \rightarrow K^- \Theta^+$  at  $P_{\text{lab}} = 1920 \text{ MeV}$  and the real part of the self-energy of  $\Theta^+$  as functions of the factor  $F$  defined in Eqs. (21) and (22) for  $J^P = 1/2^+$  (left) and  $J^P = 3/2^-$  (right). Solid, dashed and dash-dotted vertical lines show the upper limit of cross section given by the KEK experiment<sup>31,24</sup>, the limit of coupling constant, and the point where  $\text{Re}\Sigma = -100 \text{ MeV}$ .

axis denotes the factor  $F$ , which is defined by

$$g_{1/2^+}^s = F \times 0.2, \quad g_{1/2^+}^v = F \times 0.4. \quad (22)$$

As in the same way, we indicate

- cross section  $\sim 4.1 \mu\text{b}$
- lower limit of  $g_{3/2^-}^v$
- $\text{Re}\Sigma_{\Theta} = -100 \text{ MeV}$

These results, as well as the corresponding cross section for the  $K^+ p \rightarrow \pi^+ \Theta^+$  reaction are summarized in Table 9.

In Ref. 2, we have calculated the angler dependence of the differential cross sections at the energy of KEK experiment:  $P_{\text{lab}} \sim 1920 \text{ MeV}$  for  $\pi^- p \rightarrow K^- \Theta^+$  and  $P_{\text{lab}} \sim 1200 \text{ MeV}$  for  $K^+ p \rightarrow \pi^+ \Theta^+$ . The cross sections show forward peaking behavior, although the dependence is not very strong.

Table 9. Summary of the coupling constants, cross sections and self-energies.  $\sigma_{\pi^-}$  is the total cross section for  $\pi^- p \rightarrow K^- \Theta^+$  are the values at  $P_{\text{lab}} = 1920$  MeV;  $\sigma_{K^+}$  is that for  $K^+ p \rightarrow \pi^+ \Theta^+$ , which is the upper limit of the cross section at  $P_{\text{lab}} = 1200$  MeV.

$J^P$	$g^s$	$g^v$	$\sigma_{\pi^-}$ [ $\mu\text{b}$ ]	$\sigma_{K^+}$ [ $\mu\text{b}$ ]	$\text{Re}\Sigma_{\Theta}$ [MeV]
$1/2^+$	1.59	-0.27	4.1	<1928	-78
	1.37	-0.23	3.2	<1415	-58
	1.80	-0.31	5.0	<2506	-100
$3/2^-$	0.104	0.209	4.1	< 113	-23
	0.125	0.25	5.9	< 162	-32
	0.22	0.44	18	< 502	-100

Finally, we would like to briefly discuss the possible effect from the Born terms. There are reasons that the Born terms are not important in the present reactions. First, the cross sections of the Born terms are proportional to the decay width of  $\Theta^+$  and therefore suppressed if the decay width of the  $\Theta^+$  is narrow. Second, in the energy region of  $\Theta^+$  production, the energy denominator of the exchanged nucleon suppresses the contribution, especially for the  $s$ -channel term in the  $\pi^- p \rightarrow K^- \Theta^+$  reaction. Indeed, as demonstrated explicitly in Ref. 2, the effect of Born term is small enough to be neglected, for the amplitudes of the two-meson couplings studied here. However, if the experimental cross section for  $K^+ p \rightarrow \pi^+ \Theta^+$  is much smaller than we expected, the smaller coupling constants for the two-meson coupling are required. In such a case, we should consider the Born terms and interference effects more seriously.

#### 4 Summary

We have studied masses and decay widths of the baryons belonging to the octet (**8**) and antidecuplet ( $\overline{\mathbf{10}}$ ) based on the flavor SU(3) symmetry. As pointed out previously<sup>8,9,10</sup>, we confirmed again the inconsistency between the mass spectrum and decay widths of flavor partners in the **8**- $\overline{\mathbf{10}}$  mixing scenario with  $J^P = 1/2^+$ . However, the assignment of  $J^P = 3/2^-$  particles in the mixing scenario well reproduces the mass spectrum as well as the decay widths of  $\Theta(1540)$ ,  $N(1520)$ , and  $N(1700)$ . Assignment of  $3/2^-$  predicts a new  $\Sigma$  state at around 1840 MeV, and the nucleon mixing angle is close to the one of ideal mixing. The  $1/2^-$  assignment is not realistic since the widths are too large for  $\Theta^+$ . In order to investigate the  $3/2^+$  case, better experimental data of the resonances is needed.

The assignment of  $J^P = 3/2^-$  for exotic baryons seems reasonable also in a quark model especially when the narrow width of the  $\Theta^+$  is to be explained<sup>32</sup>. The  $(0s)^5$  configuration for the  $3/2^-$   $\Theta^+$  is dominated by the  $K^*N$  configuration<sup>33</sup>, which however cannot be the decay channel, since the total masses of  $K^*$  and  $N$  is higher than the mass of  $\Theta^+$ . Hence we expect naturally (in addition to a naive suppression mechanism due to the  $d$ -wave  $KN$  decay) a strong suppression of the decay of the  $\Theta^+$ .

The  $3/2^-$  resonances of nonexotic quantum numbers have been also studied in various models of hadrons. A conventional quark model description with a  $1p$  excitation of a single quark orbit has been successful qualitatively<sup>34</sup>. Such three-quark states can couple with meson-baryon states which could be a source for the five- (or more-) quark content of the resonance. In the chiral unitary approach,  $3/2^-$  states are generated by  $s$ -wave scattering states of an octet meson and a decuplet baryon<sup>35,36</sup>. By construction, the resulting resonances are largely dominated by five-quark content. These two approaches generate octet baryons which will eventually mix with the antidecuplet partners to generate the physical baryons. In other words, careful investigation of the octet states before mixing will provide further information of the inner structure of the resonances<sup>37</sup>.

In the present phenomenological study, we have found that  $J^P = 3/2^-$  seems to fit the observed data. As we have known, other identifications have been also discussed in the literature. It is therefore important to determine the quantum numbers of  $\Theta^+$  in experiments, not only for the exotic particles but also for the baryon spectroscopy of nonexotic particles. Study of high spin states in phenomenological models and calculations based on QCD are strongly encouraged.

We then studied the two-meson couplings of  $\Theta^+$  for  $J^P = 1/2^+$  and  $3/2^-$ . The effective interaction Lagrangians for the two-meson couplings were given, and these coupling constants were determined based on the  $\mathbf{8}-\mathbf{\overline{10}}$  representation mixing scheme, by using information of the  $N^* \rightarrow \pi\pi N$  decays. These values were further constrained in order to provide appropriate size of the self-energy of the  $\Theta^+$ . Finally, we have applied the effective interaction Lagrangians to the meson induced reactions  $\pi^- p \rightarrow K^- \Theta^+$  and  $K^+ p \rightarrow \pi^+ \Theta^+$ .

We have found that there was an interference effect between the two amplitudes of the scalar and vector types, which could help to explain the very small cross section for the  $\pi^- p \rightarrow K^- \Theta^+$  reaction observed at KEK<sup>24</sup>. In this case, reflecting the symmetry under exchange of two amplitudes, large cross sections for  $K^+ p \rightarrow \pi^+ \Theta^+$  reaction would be obtained as a consequence of the interference. The interference occurs in both  $1/2^+$  and  $3/2^-$  cases.

In Table 9, we have summarized the results obtained in the present analysis. For a given set of coupling constants, the upper bound of the cross sections of the  $K^+p \rightarrow \pi^+\Theta^+$  reactions were estimated by maximizing the interference effect. We observed that large cross sections of the order of millibarns for  $K^+p \rightarrow \pi^+\Theta^+$  was obtained for the  $1/2^+$  case, whereas the upper limit of the cross section was not very large for  $3/2^-$  case. Therefore, if large cross sections are observed in the  $K^+p \rightarrow \pi^+\Theta^+$  reaction, it would indicate  $J^P = 1/2^+$  for the  $\Theta^+$ .

For completeness, we would like to mention the case where the cross sections for both  $\pi^-p \rightarrow K^-\Theta^+$  and  $K^+p \rightarrow \pi^+\Theta^+$  reactions are small. If the cross section of  $K^+p \rightarrow \pi^+\Theta^+$  reaction is also small, it is not due to an interference effect, since the interference effect results in relatively large cross sections both for the two reactions. It could be explained by small coupling constants. For the  $J^P = 1/2^+$  case, both coupling constants can be zero within the experimental uncertainties. However, for the  $3/2^-$  case, there is a lower limit for the  $g_{3/2^-}^v$ , which means that the lower limit is also imposed for the cross sections. We search for the set of coupling constants that provide the minimum value for the  $K^+p \rightarrow \pi^+\Theta^+$  cross section, keeping a  $\pi^-p \rightarrow K^-\Theta^+$  cross section to be less than  $4.1\mu\text{b}$ . We obtain  $\sigma_{K^+p \rightarrow \pi^+\Theta^+} \sim 58\mu\text{b}$  with  $g_{3/2^-}^s = 0.04$  and  $g_{3/2^-}^v = 0.18$ . However, one should notice that the small coupling constants do not guarantee the dominance of two-meson coupling, and the Born terms and interference effect may play a role, which is beyond our present scope.

The present analysis provides an extension of effective interactions obtained in Ref. 12 with representation mixing and the  $J^P = 3/2^-$  case. It is also interesting to apply the present extension to the study of the medium effect of  $\Theta^{+12}$  and the production of  $\Theta^+$  hypernuclei<sup>38</sup>. From the experimental point of view, the cross section of  $K^+p \rightarrow \pi^+\Theta^+$  reaction is of particular importance to the present results. To perform a better analysis for the two-meson coupling, more experimental data for three-body decays of nucleon resonances are strongly desired.

### *Acknowledgements*

The authors would like to thank Koji Miwa, Takashi Nakano, Seung-il Nam, Eulogio Oset, Hiroshi Toki, Manuel J. Vicente Vacas, and Shi-Lin Zhu for useful discussions and comments. One of the authors (T.H.) thanks to the Japan Society for the Promotion of Science (JSPS) for support. This work supported in part by the Grant for Scientific Research [(C) No.17959600, T.H.] and [(C) No.16540252, A.H.] from the Ministry of Education, Culture, Science

and Technology, Japan.

## References

1. T. Hyodo and A. Hosaka, Phys. Rev. **D71**, 054017 (2005), hep-ph/0502093.
2. T. Hyodo and A. Hosaka, Phys. Rev. **C72**, 055202 (2005), hep-ph/0509104.
3. J. J. de Swart, Rev. Mod. Phys. **35**, 916 (1963).
4. LEPS, T. Nakano *et al.*, Phys. Rev. Lett. **91**, 012002 (2003), hep-ex/0301020.
5. NA49, C. Alt *et al.*, Phys. Rev. Lett. **92**, 042003 (2004), hep-ex/0310014.
6. D. Diakonov, V. Petrov, and M. V. Polyakov, Z. Phys. **A359**, 305 (1997), hep-ph/9703373.
7. R. L. Jaffe and F. Wilczek, Phys. Rev. Lett. **91**, 232003 (2003), hep-ph/0307341.
8. T. D. Cohen, Phys. Rev. **D70**, 074023 (2004), hep-ph/0402056.
9. S. Pakvasa and M. Suzuki, Phys. Rev. **D70**, 036002 (2004), hep-ph/0402079.
10. M. Praszalowicz, Annalen Phys. **13**, 709 (2004), hep-ph/0410086.
11. L. Y. Glozman, Phys. Rev. Lett. **92**, 239101 (2004), hep-ph/0309092.
12. D. Cabrera, Q. B. Li, V. K. Magas, E. Oset, and M. J. Vicente Vacas, Phys. Lett. **B608**, 231 (2005), nucl-th/0407007.
13. A. Hosaka, T. Hyodo, F. J. Llanes-Estrada, E. Oset, J. R. Peláez, and M. J. Vicente Vacas, Phys. Rev. **C71**, 045205 (2005), hep-ph/0411311.
14. P. Bicudo and G. M. Marques, Phys. Rev. **D69**, 011503 (2004), hep-ph/0308073.
15. T. Kishimoto and T. Sato, hep-ex/0312003.
16. F. J. Llanes-Estrada, E. Oset, and V. Mateu, Phys. Rev. **C69**, 055203 (2004), nucl-th/0311020.
17. P. Bicudo, Phys. Rev. **D70**, 111504 (2004), hep-ph/0403146.
18. F. Huang, Z. Y. Zhang, and Y. W. Yu, Phys. Rev. **C72**, 065208 (2005), hep-ph/0411222.
19. D. P. Roy, J. Phys. **G30**, R113 (2004), hep-ph/0311207.
20. T. Hyodo, A. Hosaka, and E. Oset, Phys. Lett. **B579**, 290 (2004), nucl-th/0307105.
21. W. Liu and C. M. Ko, Phys. Rev. **C68**, 045203 (2003), nucl-th/0308034.
22. Y. Oh, H. Kim, and S. H. Lee, Phys. Rev. **D69**, 074016 (2004), hep-ph/0311054.

23. Y.-s. Oh, H.-c. Kim, and S. H. Lee, Phys. Rev. **D69**, 014009 (2004), hep-ph/0310019.
24. K. Miwa *et al.* [KEK-PS E522 Collaboration], Phys. Lett. B **635**, 72 (2006), nucl-ex/0601032.
25. P. Schweitzer, Eur. Phys. J. **A22**, 89 (2004), hep-ph/0312376.
26. D. Diakonov and V. Petrov, Phys. Rev. **D69**, 094011 (2004), hep-ph/0310212.
27. J. R. Ellis, M. Karliner, and M. Praszalowicz, JHEP **05**, 002 (2004), hep-ph/0401127.
28. Particle Data Group, S. Eidelman *et al.*, Phys. Lett. **B592**, 1 (2004).
29. W. Rarita and J. S. Schwinger, Phys. Rev. **60**, 61 (1941).
30. S. I. Nam, A. Hosaka, and H. C. Kim, Phys. Lett. **B579**, 43 (2004), hep-ph/0308313.
31. K. Imai, Talk given at Exotic Hadrons workshop, May 27, 2005; [http://www.hepl.phys.nara-wu.ac.jp/exohad05/files/exohad05\\_imai.pdf](http://www.hepl.phys.nara-wu.ac.jp/exohad05/files/exohad05_imai.pdf), K. Miwa, private communication.
32. A. Hosaka, M. Oka, and T. Shinozaki, Phys. Rev. **D71**, 074021 (2005), hep-ph/0409102.
33. S. Takeuchi and K. Shimizu, Phys. Rev. **C71**, 062202 (2005), hep-ph/0410286.
34. N. Isgur and G. Karl, Phys. Rev. **D18**, 4187 (1978).
35. E. E. Kolomeitsev and M. F. M. Lutz, Phys. Lett. **B585**, 243 (2004), nucl-th/0305101.
36. S. Sarkar, E. Oset, and M. J. Vicente Vacas, Nucl. Phys. **A750**, 294 (2005), nucl-th/0407025.
37. T. Hyodo, Sourav Sarkar, A. Hosaka and E. Oset, Phys. Rev. **C73**, 035209 (2006), hep-ph/0601026.
38. H. Nagahiro, S. Hirenzaki, E. Oset, and M. J. Vicente Vacas, Phys. Lett. **B620**, 125 (2005), nucl-th/0408002.